Synthesis of Pd/Cu-Fe polymetallic nanoparticles for in situ reductive degradation of p-nitrophenol

Zhang Wenbin[*1], Liu Lanyu[1], Zhao Jin[1], Gao Fei[1], Wang Jian[1] and Fang Liping[2]

[1]*Ecological and Environmental Monitoring Center of Chongqing, Chongqing 401147*
[2]*China University of Geosciences, No. 388, Lumo Road, Wuhan 430074, China*

Abstract. With a small particle size, specific surface area and chemical nature, Pd/Cu-Fe nanocomposites can efficiently remove the organic compounds. In order to understand the applicability for in situ remediation of contaminated groundwater, the degradation of p-nitrophenol by Pd/Cu-Fe nanoparticles was investigated. The degradation results demonstrated that these nanoparticles could effectively degrade p-nitrophenol and near 90% of degradation efficiency was achieved by Pd/Cu-Fe nanocomposites for 120 min treatment. The efficiency of degradation increased significantly when the Pd content increased from 0.05 wt.% and 0.10 wt.% to 0.20 wt.%. Meanwhile, the removal percentage of p-nitrophenol increased from 75.4% and 81.7% to 89.2% within 120 min. Studies on the kinetics of p-nitrophenol that reacts with Pd/Cu-Fe nanocomposites implied that their behaviors followed the pseudo-first-order kinetics. Furthermore, the batch experiment data suggested that some factors, including Pd/Cu-Fe availability, temperature, pH, different ions (SO_4^{2-}, PO_4^{3-}, NO_3^-) and humic acid content in water, also have significant impacts on p-nitrophenol degradation efficiency. The recyclability of the material was evaluated. The results showed that the Pd/Cu-Fe nanoparticles have good recycle performance, and after three cycles, the removal rate of p-nitrophenol is still more than 83%.

Keywords: Cu/Fe; degradation; iron; nanoparticles; p-nitrophenol; reduction

1. Introduction

As an important chemical raw material, p-nitrophenol is commonly applied in pesticides, pharmaceuticals, dielectric and biocides and other industrial and agricultural production, which causes serious environmental problem in recent years (Adekola *et al.* 2017). Owing to its high toxicity, wide distribution, carcinogenic, and biorefractory, p-nitrophenol is listed as the priority pollutant by the USEPA. It has been reported that the negative effects of p-nitrophenol on the environment and humans could last for a long time by Abd El Maksod and Saleh (2010). Once being released into both the ground and surface water, p-nitrophenol will accumulate the transformation in the surrounding ecosystems, and could damage the liver, kidney, blood, and nervous systems of human and animals. Therefore, it is necessary to search for some methods to remove p-nitrophenol from the environment effectively.

Nanoscale zero valent iron (nZVI) and bimetallic nanoparticles (NPs, e.g. Pd/Fe, Ni/Fe, Cu/Fe etc.) have attracted significant attention in the last decade for its highly efficient degradation of contaminants, including nitro aromatic compounds (Hamidreza *et al.* 2020). nZVI possesses large specific surface area and high reactivity, and is widely used in in-situ groundwater treatment (Cervantes *et al.* 2016). On the contrary, it has been revealed that nZVI is easily oxidized and tends to aggregate

rapidly for the vander Waals and magnetic forces, which results in only partial degradation and deficient reactivity for the complicated organic compounds (Wang *et al.* 2014). Several studies have exhibited that depositing a certain amount of catalytic metals such as *Pt*, *Cu*, and *Pd* on the nZVI surface could form various bimetallic and polymetallic nanoparticles. The reactivity of nZVI has been further enhanced for the degradation of nitro compounds in water by Li and Chen (2013). The bimetallic Cu/Fe and polymetallic Pd/Cu-Fe nanoparticles are preferred options especially for groundwater remediation, because they display obvious advantages such as high degradation rate, mild hydrogenation rate and low environmental hazard.

In this letter, the successful synthesis of palladium-copper-iron nanoparticles with an average diameter of less than 50 nm wereas reported. The first attempt was to investigate the removal efficiency of p-nitrophenol in aqueous solutions under a wide range of conditions, including pH, temperature and Pd content. Moreover, the catalytic performance and reusability were explored. In addition, different background ions on the reductive degradation of p-nitrophenol were also studied. Finally, the mechanisms of degradation and the degradation path were investigated as well.

2. Experiment

2.1 Synthesis of Cu/Fe and Pd/Cu-Fe nanoparticles

Pd/Cu-Fe NPs were used in this study and prepared using well known liquid-phase method in a 250 mL

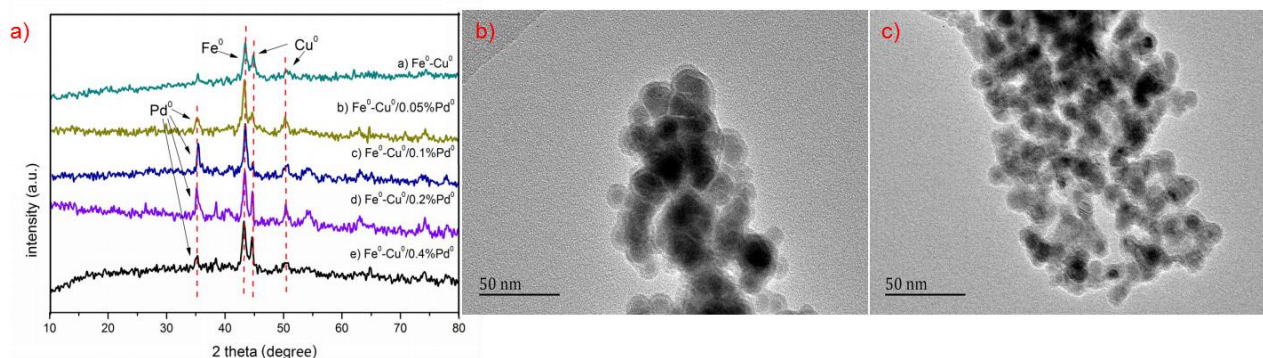∗Corresponding author, Ph.D.,
 E-mail: 307526489@qq.com

Fig. 1 *XRD* patterns of different palladium content *Pd/Cu-Fe* polymetallic NPs (a), TEM images of *Cu/Fe* polymetallic NPs (b), TEM images of Pd/Cu-Fe polymetallic NPs (c)

three-necked flask (Lai *et al*. 2014a). Briefly, 0.1M $FeCl_3 \cdot 7H_2O$ and $CuSO_4 \cdot 5H_2O$ were dissolved into ethanol solution (30%volume) under N_2 flush with mechanical stirring. On the other hand, 0.3M borohydride solution was slowly dropped into the above mixture by syringe and stirred for 30 min at room temperature. The solution color changed from bluish green to light green, then brown and finally dark. A small amount of black iron-copper bimetallic nanoparticles precipitated at the bottom of the centrifuge tube. The content of Cu in Cu/Fe nanoparticles was 41%, and then an aqueous solution of palladium acetate was added dropwise. As the synthesized metal NPs were washed with O_2-free deionized water and ethanol several times, followed by being vacuum-dried in a desiccator and stored in the pasorina for further use.

2.2 Characterization of nanoparticles

The morphology and size of the particles were observed with a Tecnai G220 transmission electron microscopy (TEM) (FEI, Netherlands). The composition and crystal structure of particles were examined by a D/max2200 X-ray diffractometer（XRD）(Rigaku Corp. Japan) with CuKα radiation (λ = 1.5418 nm) that operates at an accelerating voltage of 45 *KV* in a step scanning mode, with a step size of 0.02 and a counting time of 1s per step in the range of 10-80º.

2.3 Batch degradation experiments

The batch experiments were performed in 100 ml serum vials as the batch reactor system and capped with Teflon septa. The desired volumes of p-nitrophenol stock solutions and a certain amount of deoxygenated deionized water were added into the serum bottles that contain freshly prepared Pd/Cu-Fe nanoparticles, which resulted in an initial p-nitrophenol concentration of 30 mg/L. Then, the bottles were placed on a rotary shaker shaken at 200 rpm at temperature of 298 ± 1 K. The aliquots of samples were collected with the glass syringes at specified times and the reaction was quenched by passing through 0.22 m filter membrane to remove the unreacted particles. Acetonitrile was purchased from Shanghai Jing Purification Technology Co. Ltd., and it is chromatographically pure, without any

purification treatment before application. All other chemicals used in this study were purchased from Shanghai Aladdin Biochemical Technology Co. Ltd., and were analytically graded and used without further refinement.

2.4 Analytical methods

P-nitrophenol and its degradation products were analyzed using HPLC system (Agllent 1100 serves, gradient pump and degasser, Agilent Technologies, Germany). The mobile phase was a mixture of acetonitrile (chromatographic purity) and phosphoric acid (pH = 3.0) (60/40, v/v) in an isocratic system at a flow rate of 0.8 mL/min, injection volume of 10μl, and UV detector of 317 nm. The adsorption capability (qe) was calculated by the following equations (Wang *et al*. 2013):

$$q_e = \frac{(c_0 - c_e)V}{m} \tag{1}$$

where C_0 represents the initial concentration of p-nitrophenol solution (mg/L), C_e means the equilibrium concentration of p-nitrophenol solution (mg/ L), V marks the total volume of solution (mL), and m stands for the nanoparticles dosage (mg).

3. Results and discussion

3.1 Characterization of nanoparticles

X-ray powder diffraction (XRD) pattern and TEM image of freshly prepared *Pd/Cu-Fe* nanoparticles are given in Fig. 1. The sharp diffraction peak of 2θ = 44.70° is the characteristic peak of α-Fe crystal phase (Heydari *et al* 2019). The diffraction peaks at the 2θ values of 46.20° and 50.42° are the characteristic peaks of the zero valent copper that correspond to the (110) and (200) (220) crystal planes of the cubic copper crystals, respectively (Ma *et al*. 2015). The intense peaks at 2θ = 35.58° confirmed the presence of palladium nanoparticle (Luo *et al*. 2016, Jaehyun *et al* 2020). The peaks of ferrous oxide, iron oxide and other oxides were not discovered in the figure, indicating that the synthesized nanoparticles were better crystallized with
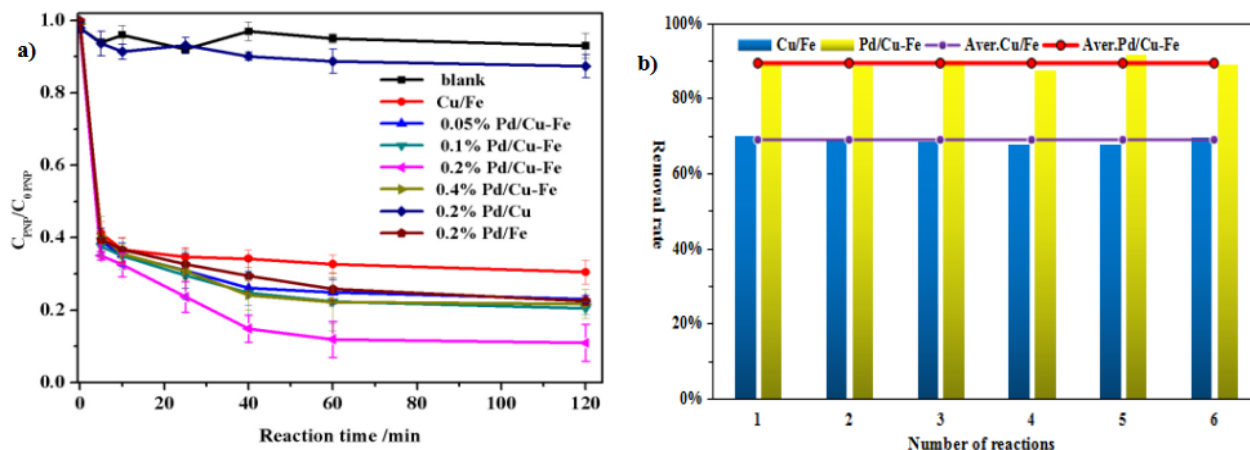
Fig. 2 p-nitrophenol degradation by *Pd/Cu-Fe* polymetallic NPs (a), reproducibility experiments (b), experimental conditians: 0.15 g.L-1 Pd/Cu-Fe-0.2%, 30 mg.L-1 p-nitrophenol

higher purity. The TEM image demonstrated that the synthesized *Pd/Cu-Fe* polymetallic particles aggregated and agglomerated for the molecules of vander Waals force and magnetic interactions between the metallic. The *Cu/Fe* nanoparticles were composed of spherical particles with a particle size of about 30 nm to 50 nm. However, the fresh *Pd/Cu-Fe* nanoparticles were also spherical, but the particle size ranges from 20 to 30 nm due to the introduction of palladium atoms, thus weakening the agglomeration between particles, and enhancing the dispersion of nanoparticles in water (Wang *et al*. 2013, Rouhullah *et al* 2018).

3.2 Effect of Pd loading (wt%) on the degradation of p-nitrophenol

The degradation of halogenated organic compounds is very effective to accelerate the catalytic degradation reaction by coating the appropriate amounts of Pd on the surface of Cu/Fe bimetallic nanoparticles. Therefore, the Pd loading percentage on Cu/Fe nanoparticles may be one of the important influential factors on the reductive degradation efficiency. Fig. 2(a) shows the p-nitrophenol degradation by different specified Pd/Cu-Fe nano- composites with various Pd loadings. It can be clearly seen that the efficiency of catalytic degradation was obviously increased as Pd content over Cu/Fe bimetallic nanoparticles increased from 0, 0.05, and 0.1 to 0.2 wt%. When the palladium content was 0.2%, the Pd/Cu-Fe polymetallic catalyst had the strongest reactivity, and the removal rate of p-nitrophenol was nearly 90% within 120 min at room temperature, which was 20.8% higher than that of p-nitrophenol using Cu/Fe nanoparticles under the same conditions. The loading of Pd would reduce the activation energy and increase the number of activated molecules of the reaction, and allow more interactions between the catalysts and pollutants, thus increasing the reaction efficiency (Wang *et al*. 2014). However, the continuing increase in the palladium content over Cu/Fe nanoparticles from 0.2 to 0.4 wt% resulted in the slight decrease in the removal efficiency of p-nitrophenol. It could be the accumulation of excessive hydrogen gas as the

degradation reaction proceeds, which inhibits the effective contact between the target organic pollutants and metal catalyst materials and resultantly decreases the surface area availably for p-nitrophenol degradation (Ali *et al*. 2019). On the other hand, excess palladium atoms caused the overlapping between palladiumr atoms and covered the nanoparticles that conserved active sites, thus reducing the reactivity and decreasing the removal rate of p-nitrophenol, which is similar to the previously reported studies (Wang *et al*. 2016). The optimal palladium content was selected at about 0.2 wt% for efficient degradation with minimal palladium application.

Six times of denitration experiments were conducted using Cu/Fe and Pd/Cu-Fe particles under the same conditions. The experimental results are listed in Fig. 2(b). The Cu/Fe and Pd/Cu-Fe degradation of p-nitrophenol had good reproducibility. The average results of the six experiments were 68.9% and 89.4%, and the ranges of relative standard deviation were 1.4% and 1.6%, respectively.

3.3 Effect of initial pH on the degradation of p-nitrophenol

The pH is considered as one of the important factors affecting the degradation efficiency of p-nitrophenol by Pd/Cu-Fe nanoparticles. In this study, the initial pH of the reactant solution was adjusted using 0.1 mol/L hydrochloric acid and 0.1 mol/L sodium hydroxide solution. The effects of different initial pH values on the catalytic degradation of p-nitrophenol by Pd/Cu-Fe nanoparticles are displayed in Fig. 3(a). The acidic environment is favorable for the degradation of p-nitrophenol. The alkaline condition is not conducive to the degradation reaction. When the initial pH value was 3.0, the removal rate of p-nitrophenol in the solution was 94.3% after the reaction for 120 min. The pH continued to increase from 5, 7 to 9, and the degradation percentages of p-nitrophenol obviously dropped from 91.7% and 89.2% to 73.8%, respectively, which indicated that the large amount of H^+ present in the low pH solution accelerates the corrosion of zero valent iron and enables
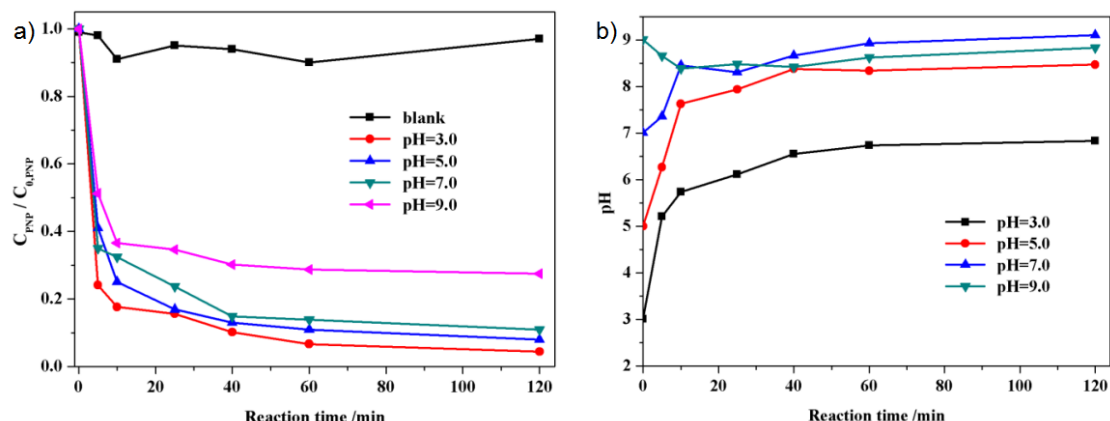
Fig. 3 Effect of initial pH on the removal of p- nitrophenol (a), change of pH over time during the denitration course (b), experimental conditians: 0.15 g.L^{-1} *Pd/Cu-Fe*-0.2%, 30 mg.L^{-1} p- nitrophenol

more iron surface to remain available, which provides lots of active sites required for the reaction with the nitrolated molecules (Ali *et al.* 2018). At higher pH values, the presence of a large amount of OH$^-$ in the reactant solution and the formation of Fe^{3+} after the formation of ferric hydroxide precipitation deposited on the surface of nanoparticles, thereby reducing the p-nitrophenol effective contraction with the catalyst surface active site and the removal efficiency of p-nitrophenol (Cervantes *et al.* 2016).

The change of pH over time during the denitration course is shown in Fig. 3(b). Acidic and neutral initial pH values resulted in a gradual increase in pH over time, which means that protons are consumed during the reaction (Chen *et al.* 2018). The alkaline initial pH caused the pH to decline slowly for the first 20 minutes and then kept stable, because Fe (II) or Fe (0) surfaces in aqueous solutions can consume part of the hydroxide ion (Yuan *et al.* 2017, Rouhllah *et al.* 2018).

3.4 Influence of humid acid and different ions (NO$_3^-$, SO$_4^{2-}$ and PO$_4^{3-}$) on the p-nitrophenol removal by Pd/Cu-Fe nanocomposites

The effects of humic acid and different ions (NO$_3^-$, SO$_4^{2-}$ and PO$_4^{3-}$) on the catalytic performance of Pd/Cu-Fe nanoparticles were studied by selecting the humid acid and NaNO$_3$, Na$_2$SO$_4$ and Na$_3$PO$_4$ solution as a reagent, and the influences of Na$^+$ can be ignored due to the less effects of degradation efficiency on p-nitrophenol. As shown in Fig. 4, in general, the removal rate ofp-nitrophenol decreases with the increase of the concentration of background ions. Humid acid has modest inhibitory effects on the degradation rate of p-nitrophenol by Pd/Cu-Fe nano-particles. The humic acid concentration increases from 0, 5, 10, and 20 to 50 mg/L, thus leading to the decrease in p-nitrophenol degradation rate from 89.2%, 85.6%, 82.4%, and 80.1% to 78.3% in 120 min. This trend could be attributed to the accumulation of adsorbed humic acid on Pd/Cu-Fe nanoparticles surface, which may reduce the p-nitrophenol degradation rate (Cao *et al.* 2011). The Fe^{2+} is produced by the corrosion of the zero valent iron and the humic acid interaction presents in the solution. The competitive

adsorption between the HA and the pollutant occupies the active site of nanopartiles surface and inhibits iron corrosion. (Lai *et al.* 2014b, Scott 1998).

Fig. 4(b) shows the effects of different concentrations of NO$_3^-$ on p-nitrophenol. removal rates. When the concentration of NO$_3^-$ increased from 0, 5, and 10 to 20 mg/L, the degradation rate of p-nitrophenol decreased to 89.2%, 87.2%, 85.9% and 83.0%, respectively. However, the concentration of NO$_3^-$ in the reaction solution continues to increase to 50 mg/L-1, and the removal rate of p-nitrophenol is slowly increased to 83.3%, because the low concentration of NO$_3^-$ is adsorbed on the surface of the catalyst and the contaminants compete with the reactive sites of the catalyst, thereby reducing the contaminant and catalyst contact, which is detrimental to the degradation reaction (Ma *et al.* 2015). On the other hand, a satisfactory etchant, NO$_3^-$ can attack *Pd/Cu-Fe* nanoparticles surface passivation oxide layer, which is conductive to maintaining a fresh catalyst interface, so that p-nitrophenol and nano-particles are more effectively contacted, thus eventually affecting the p-nitrophenol reduction (Anjali *et al.* 2019).

Different contents of sodium sulfate were added to the reaction solution. After the reaction for 360 min, the effects of the sulfate ion on the degradation of p-nitrophenol by Pd/Cu-Fe were investigated. As seen from Fig. 4(c), it is clear that the addition of sulfate concentration prevents the catalytic reduction of p-nitrophenol. When the initial reaction concentration of sulfate increases from 0, 5, and 10 to 50 mg/L, the removal rate of corresponding p-nitrophenol is gradually decreased from 89.2%, 87.0% and 83.7% to 81.3%. The sulfate ion is easily reduced to elemental sulfur and lead to the catalyst poisoning and activity losing, and the catalytic weakens. At the same time, sulfate ions are adsorbed on the catalyst surface, and occupy lots of active sites, thus causing catalytic incomplete and inefficient p-nitrophenol. (Ali Heidari *et al.* 2018a).

The concentration effects of PO$_4^{3-}$ on the degradation of p-nitrophenol by *Pd/Cu-Fe* nanoparticles were further examined. Fig. 4(d) illustrated that the existence of PO$_4^{3-}$ has significant impacts on p-nitrophenol degradation efficiency. With the increase of phosphate content, the removal percentage of p-nitrophenol is dramatically
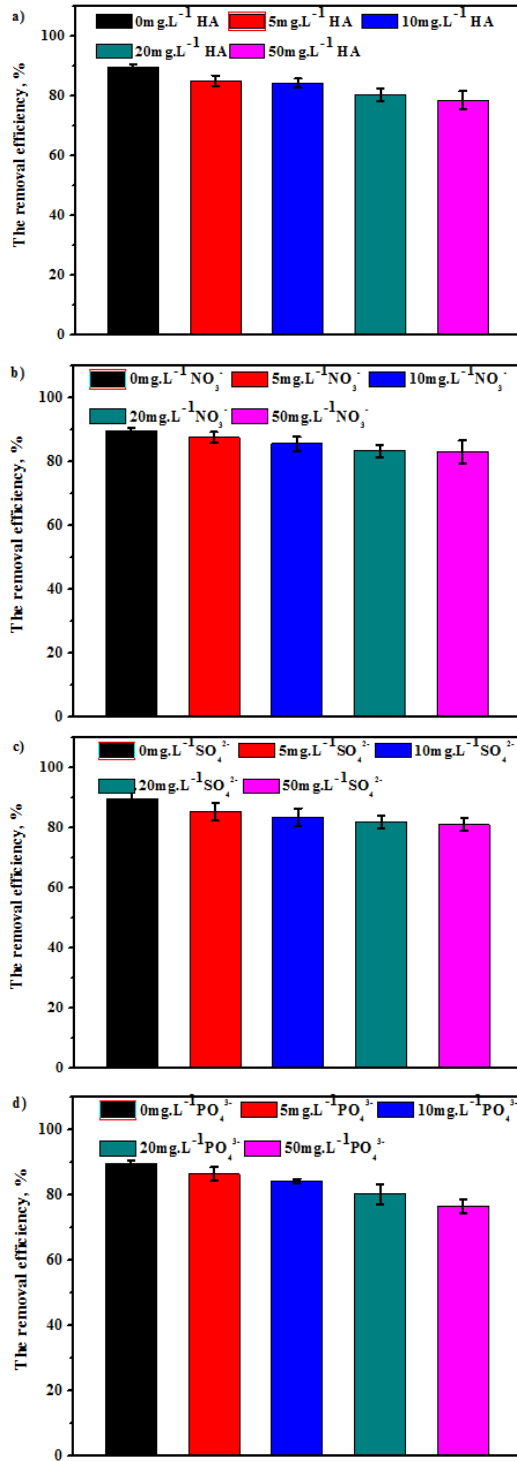
Fig. 5 Reusability of *Pd/Cu-Fe* for p-nitrophenol, Experimental conditians: 0.15 g.L^{-1} *Pd/Cu-Fe*-0.2%, 30 mg.L^{-1} p-nitrophenol

weakening the adsorption of the catalyst to the contaminants and catalytic performance, and inhibiting the removal of p-nitrophenol rapidly (Luo *et al.* 2016).

3.5 Reusability of Pd/Cu-Fe nanocomposites

The reusability of Pd/Cu-Fe for p-nitrophenol removal is displayed in Fig. 5. According to the figure, the removal rate of p-nitrophenol was as high as 88.7% in the first run. The Pd/Cu-Fe particles can be easily collected by a magnet. With the progress of the degradation reaction, the catalytic activity of *Pd/Cu-Fe* decreases with the consumption of zero-valent iron and possible aggregation. After two cycles, the removal rate of p-nitrophenol is still more than 83%. The decreased reactivity can be explained by the depletion of ZVI and the possible accumulation of Pd/Cu-Fe particles.

3.6 Kinetics and thermodynamics study of p-nitrophenol degradation

Catalytic kinetic is one of the most important indicators to reflect the catalytic efficiency of the catalyst, which determines the potential application value of the catalyst to a great extent (Chen *et al.* 2018). In order to describe the dynamic behavior and explore the degradation mechanism, the degradation kinetic can be elucidated by the pseudo-first-order and pseudo-second-order dynamical models. The linear expression of these kinetic models can be provided as following equations by Park and Bae (2018):

$$\ln\left(q_e - q_t\right) = \ln q_e - kt \qquad (2)$$

$$q_t = \frac{k_2 q_e^2 t}{1 + k_2 q_e t} \qquad (3)$$

where q_t (mg/g) is the adsorption capability concentration of the p-nitrophenol vary with time t (min), q_e (mg/g) marks the equilibrium adsorption capability of the p-nitrophenol, and k_1 (min^{-1}) and k_2 (g.mg^{-1}.min^{-1}) are the pseudo-first-order and pseudo-second-order model rate constants, respectively. The two kinetic modes fitting for catalytic degradation of p-nitrophenol with different materials are

Fig. 4 Effect of (a) humic acid, (b) NO$_3^-$ (c) SO$_4^{2-}$ and (d) PO$_4^{3-}$, Experimental conditians: 0.15 g.L^{-1} *Pd/Cu-Fe*-0.2%, 30 mg.L^{-1} p- nitrophenol

decreased. When the PO$_4^{3-}$ concentration increased to 10, 20 and 50 mg•L^{-1}, the removal rate of p-nitrophenol decreased to 82.3%, 79.5% and 76.6%, respectively, compared with the decrease of blanks by 6.9%, 9.7% and 12.6%, because the formation of phosphoric acid precipitates on the surface of the nanoparticles, and occupies and deactivates the active sites required for the reaction, thereby
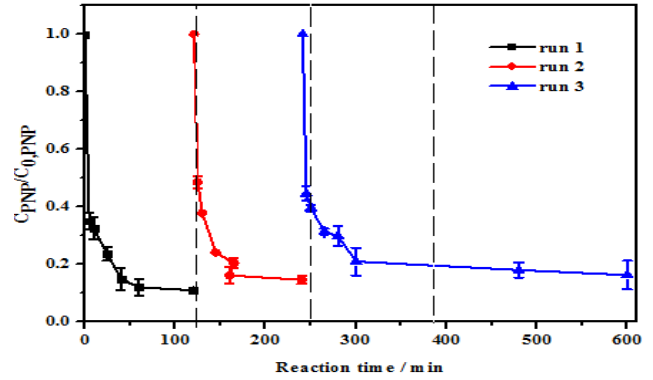
Table 1 p-nitrophenol kinetic parameters of adsorption kinetic models

Material	pseudo-first-order kinetic model				pseudo-second-order kinetic model		
	q_{exp} (mg.g^{-1})	k_1 (min^{-1})	$q_{cal,1}$ (mg.g^{-1})	R^2	k_2 (g.mg^{-1}.min^{-1})	$q_{cal,2}$ (mg.g^{-1})	R^2
Cu-Fe	139.1	0.05725	129.4	0.9565	0.0034	117.3	0.9534
0.05%Pd/Cu-Fe	153.9	0.06914	149.7	0.9670	0.0040	97.5	0.9437
0.1%Pd/Cu-Fe	159.0	0.07296	144.4	0.9465	0.0041	123.6	0.9328
0.2%Pd/Cu-Fe	178.8	0.08133	154.7	0.9745	0.0051	143.2	0.9465

*Table 1 observed that the pseudo-first-order model presents a higher correlation coefficient than pseudo- second-order. Experimental conditians: 30mg.L-1 p-nitrophenol, 0.15g/L nanoparticles
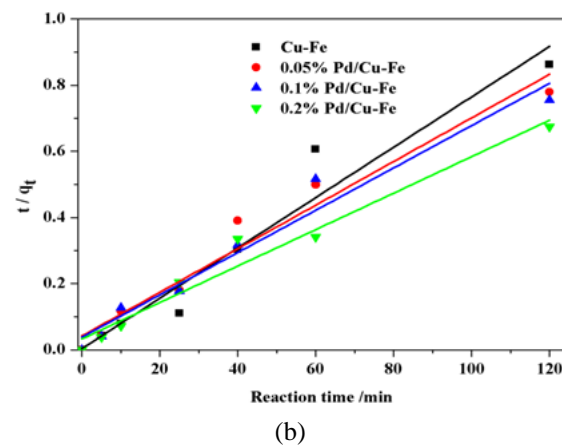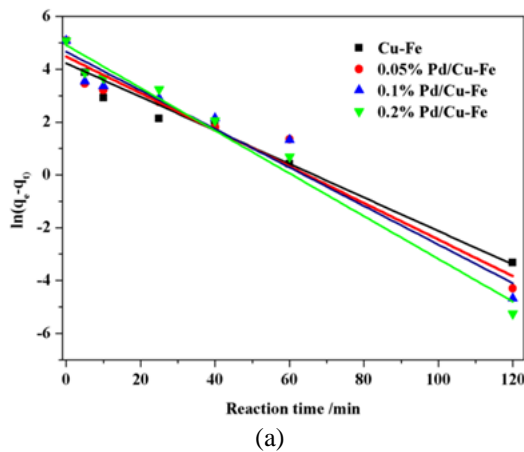

Fig. 6 (a) pseudo-first-order kinetic plot and (b) pseudo-second-order kinetic plot for removal of p-nitrophenol, Experimental conditians: 30 mg.L-1p-nitrophenol

illustrated in Fig. 6. The two kinetic model rate constant k_1 and k_2, the theoretically calculated equilibrium concentration ($q_{e,cal,1}$, $q_{e,cal,2}$), along with the correlation co-efficient R^2 of pseudo-first-order and pseudo-second- order are listed in Table 1. From the results, it is obvious that the pseudo-first-order model presents a higher correlation coefficient for p-nitrophenol degradation process. The theoretically calculated equilibrium capacity ($q_{e,cal,1}$) from the pseudo-first-order model is closer to the experimental results ($q_{e,exp}$) than that form the pseudo- second-order model. Thus, it was concluded that the pseudo-first-order model fitted the degradation experiment. In addition, it shows that k_1 value for p-nitrophenol degradation increased dramatically from 0.05725, 0.06914, and 0.07296 to 0.08133 min^{-1}, as the palladium content increased from 0%, 0.05%, and 0.1% to 0.2%. The degradation capability of the p-nitrophenol (qe) also followed an order Pd/Cu-Fe (0.2%) > Pd/Cu-Fe (0.1%) > Pd/Cu-Fe (0.05%) > Cu/Fe, which was consistent with the previous results.

The pseudo-first order linear fitting curves for the removal of p-nitrophenol at different temperatures are displayed in Fig. 7. Table 2 lists the relevant fitting parameters and the error function values (R^2). It can be clearly discovered that the pseudo-first-order rate constants k of p-nitrophenol from Pd/Cu-Fe NPs increases from 0.08133 min^{-1} to 0.08751 min^{-1} as the reaction temperature rises from 298 K to 318 K. High temperature is beneficial to the degradation by metal nanoparticles, which is also observed by other researchers (Lai *et al*. 2014a). The activation energy E_a can be determined from the following

equation:

$$\ln k_{obs} = \frac{E_a}{RT} - \ln A \qquad (4)$$

where k_{obs} is the measured first-order-rate constant, A means a frequency factor, R stands for ideal gas constant, and T represents temperature. A plot of ln$k$ versus $1/T$ is shown in Fig. 7(c). The activation energy of the degradation of p-nitrophenol by *Pd/Cu-Fe* particles is approximately 2.9 kJ/mol. The activation energy decrease (10.9 kJ/mol) in this study is much more, compared with the Cu/Fe bimetallic system (13.8 kJ/mol), which is in line with previous studies (Lien. *et al*. 2007). The partial removal of nitro-compounds was observed for Cu/Fe, whereas the full removal was observed for Fe coupled with good hydrogenation metal catalyst such as Pd, Ag and Ni (Anjali *et al*. 2019a). The fast electronic transfer from iron to Cu and Pd plays an important role in the galvanic corrosion model (Ali *et al*. 2019). According to the previous studies, the degradation pathway of p-nitrophenol mainly degrades into by direct reduction on catalytic activity site or indirect reduction of [H]$_{abs}$, which is finally reduced to p-aminophenol. Obviously, the p-aminophenol is usually observed during the degradation of p-nitrophenol, while the degradation intermediate (nitrouso-phenol) is hard to be detected in this work (Yuan *et al*. 2017). When it was produced in the treatment and similar observation was also reported by other researchers, nitrouso-phenol might be quickly reduced into p-aminophenol (Lai *et al*. 2014a, Wang *et al*. 2013).

Table 2 p-nitrophenol kinetic parameters of pseudo-first-order and ln$k \sim 1/T$ models

Temperature	pseudo-first-order kinetic model				ln$k \sim 1/T$		
	q_{exp}	k_1	$q_{cal,1}$	R^2	$1/T$	ln$k$	R^2
(K)	(mg.g^{-1})	(min^{-1})	(mg.g^{-1})		(K^{-1})		
298	178.8	0.08133	174.5	0.9653	0.003356	-2.5096	
308	185.7	0.08398	185.6	0.9501	0.003247	-2.4772	0.99728
318	193.2	0.08751	203.2	0.9687	0.003145	-2.4362	

*Table 2 observed that increasing the temperature is beneficial to the degradation for p-nitrophenol. Experimental conditians: 0.15g.L^{-1} *Pd/Cu-Fe*-0.2%,30mg.L^{-1} p-nitrophenol
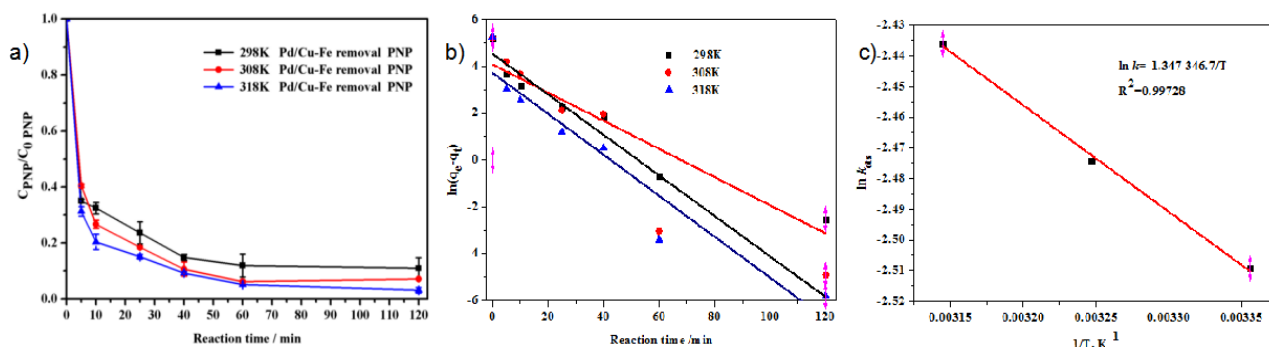

Fig. 7 Effect of temperature on the removal of p-nitrophenol by *PdCu/Fe* (a), pseudo-first-order kinetics fitting (b), ln$k \sim 1/T$ model fitting. Experimental conditians: 0.15g.L^{-1} *Pd/Cu-Fe*-0.2%,30 mg.L^{-1}p-nitrophenol
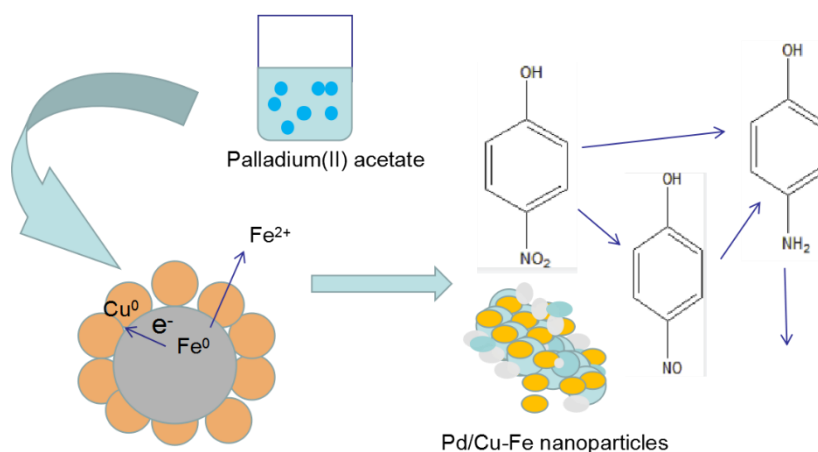

Fig. 8 Proposed mechanism for p-nitrophenol degradationusing Pd/Cu-Fe nanoparticles

4. Conclusions

In summary, with less than 20nm in diameter, Pd/Cu/Fe polymetallic nanoparticles were successfully prepared by water-phase approach and utilized for in situ remediation of p-nitrophenol. This study proved that the introduction of palladium metal to construct Pd/Cu/Fe composite nano-particles can effectively improve the catalytic degradation of p-nitrophenol that is contained in the water at room temperature and atmospheric pressure. The retrievability of Pd/Cu/Fe particles was confirmed over three consecutive recycles. The existence of different background ions in the reaction solution has significant impacts on p-nitrophenol degradation efficiency. In the range of concentration, p-nitrophenol removal percentages gradually decreased with the increase of humic acid, PO_4^{3-}, SO_4^{2-} and NO_3^- concentration, and the inhibitory effects followed an order of $PO_4^{3-} > HA^- > SO_4^{2-} > NO_3^-$, which is of great importance, because it helps us to better understand the inhibitory mechanisms of background ions. Most importantly, the exploration of the effects of nanoparticles on the remediation of contaminated soil and groundwater in the future is significant.

Acknowledgement

References

Abd El Maksod, I.H. and Saleh, T.S. (2010), "The use of nano supported nickel catalyst in reduction of p-nitrophenol using hydrazine as hydrogen donor", *Green Chem. Lett. Rev.*, **3**(2), 127-134. https://doi.org/10.1080/17518251003596143.

Adekola, F.A., Orimolade, B.O. and Adebayo, G.B. (2017), "Removal of p-nitrophenol from aqueous solution using synthesized silica-magnetite composite", University of Ilorin, Ilorin, Naigeria.

Ali, Z.I., Bekhit, M., Sokary, R. and Afify, T.A. (2019), "Radiation synthesis of copper sulphide/poly(vinyl alcohol) nano- composites films: An efficient and reusable catalyst for p-nitrophenol reduction", *Int. J. Environ. An. Ch.*, **99**(13), 1313-1324. https://doi.org/10.1080/03067319.2019.1619717.

Anjali, M.S., Shrihari, S. and Sunil, B.M. (2019), "Potential valorisation of ferrous slag in the treatment of water and wastewater: A review", *Adv. Environ. Res.*, **8**(1), 55-69. http://doi.org/10.12989/aer.2019.8.1.055.

Cervantes, F.J., Rodriguez-Lopez, J.L. and Pena-Martinez, M. (2016), "Enhanced Reduction of p-nitrophenol by a methanogenic consortium promoted by metallic nanoparticles", *Water Air Soil Pollut.*, **227**(10), https://doi.org/10.1007/s11270-016-3058-x.

Chen, R.F., Yang, L.P. and Guo, Y.K. (2018), "Effect of p-nitrophenol degradation in aqueous dispersions of different crystallized goethites", *Photochem. Photobiol.*, **353**(2), 337-343. http://doi.org/10.1016/j.jphotochem.2017.11.028.

Heidari, A., Keikha, R., Haghighi, M.S. and Hosseinabadi, H. (2018), "Numerical study for vibration response of concrete beams reinforced by nanoparticles", *Struct. Eng. Mech.*, **67**(3), 311-316. http://doi.org/10.12989/sem.2018.67.3.311.

Jung, J., Sibag, M., Shind, B. and Cho, J. (2020), "Experimental investigation of organic fouling mitigation in membrane filtration and removal by magnetic iron oxide particles", *Membr. Water Treat.*, **11**(3), 223-229. http://doi.org/10.12989/mwt.2020.11.3.223.

Lai, B., Zhang, Y.H. and Chen, Z.Y. (2014a), "Removal of p-nitrophenol (PNP) in aqueous solution by the micron-scale iron-copper (Fe/Cu) bimetallic particles", *Appl. Catal. B Environ.*, **144**, 816-830. http://doi.org/10.1016/j.apcatb.2013.08.020.

Lai, B., Zhang, Y.H. and Li, R. (2014b), "Influence of operating temperature on the reduction of high concentration p-nitrophenol (PNP) by zero valent iron (ZVI)", *Chem. Eng. J.*, **249**, 143-152. http://doi.org/10.1016/j.cej.2014.03.108.

Li, M.L. and Chen, G.F. (2013b), "Revisiting catalytic model reaction p-nitrophenol/NaBH4 using metallic nanoparticles coated on polymeric spheres", *Nanoscale*, **5**(23), 11919-11927. http://doi.org/10.1039/c3nr03521b.

Lien, H.L. and Zhang, W.X. (2007a), "Nanoscale Pd/Fe bimetallic particles: Catalytic effects of palladium on hydro-dechlorination", *Appl. Catal. B Environ.*, **77**(1), 110-116. https://doi.org/10.1016/j.apcatb.2007.07.014.

Luo, M.H., Xia, K.J., Zhou, G.H. and Ge, W. (2016), "Synthesis of Pd/PEI-GNs composites as electrocatalyst for reduction of p-nitrophenol", *Chem. J. Chinese U.*, **37**(12), 2268-2274. http://doi.org/10.7503/cjcu20160338.

Ma, C., Chen, Y. and Chen, J. (2015), "Surfactant-assisted preparation of FeCu catalyst for Fischer-Tropsch synthesis", *J. Brazil. Chem. Soc.*, **26**(7),1520-1526. https://doi.org/10.5935/ 0103-5053. 20150121.

Park, J. and Bae, S. (2018), "Formation of Fe nanoparticles on water-washed coal fly ash for enhanced reduction of p-nitrophenol", *Chemosphere*, **202**, 733-741. http://doi.org/10.1016/j.chemosphere.2018.03.152.

Rashidi, H., Sulaiman, N.M.N., Hashim, N.A., Bradford, L.,

Asgharnejad, H. and Larijani, M.M. (2020), "Development of the ultra/nano filtration system for textile industry wastewater treatment", *Membr. Water Treat.*, **11**(5), 333-334. http://doi.org/10.12989/mwt.2020.11.5.333.

Rouhllah, D., Mohammad, B.M., and Abbas, Z. (2018), "Evaluation of raw wastewater characteristic and effluent quality in Kashan Wastewater Treatment Plant" *Membr. Water Treat.*, **9**(4), 273-278. http://doi.org/10.12989/mwt.2018.9.4.273.

Scott, D.T., McKnight, D.M., Blunt-Harris, E.L., Kolesar, S.E. and Lovley, D.R. (1998), "Lovley, Quinonemoieties act as electron acceptors in the reduction of humic substances by humics- reducing microorganisms", *Environ. Sci. Technol.*, **32**(1), 57-62. http://doi.org/10.1080/15533174.2012.684258.

Sullivan, P., Agardy, F.J. and Clark, J.J. (2005), *The Environmental Science of Drinking Water*, Butterworth-Heinemann, Oxford, U.K.

Tang, J., Tang, L. and Feng, H.P. (2016), "pH-dependent degradation of p-nitrophenol by sulfidated nanoscale zero valent iron under aerobic or anoxic conditions", *J. Hazard. Mater.*, **320**, 581-590. http://doi.org/10.1016/j.jhazmat.2016.07.042.

Wang, T.C., Qu, G.Z., Li, J. and Liang, D.L. (2014), "Remediation of p-nitrophenol and pentachlorophenol mixtures contaminated soil using pulsed corona discharge plasma", *Sep. Purif. Technol.*, **122**, 17-23. http://doi.org/10.1016/j.seppur.2013.10.043

Wang, X., Zhu, M. and Liu, H. (2013), "Modification of Pd–Fe nanoparticles for catalytic degradation of 2,4-dichlorophenol", *Sci. Total Environ.*, **449**, 157-167. http://doi.org/10.1016/j.scitotenv.2013.01.008.

Wang, X.Y., Xing, D.F. and Ren, N.Q. (2016), "p-nitrophenol degradation and microbial community structure in a biocathode bioelectrochemical system", *Rsc Adv.*, **6**(92), 89821-89826. http://doi.org/10.1039/c6ra17446a.

Yuan, Y., Yuan, D.H. and Zhang, Y.H. (2017), "Exploring the mechanism and kinetics of Fe-Cu-Ag trimetallic particles for p-nitrophenol reduction", *Chemosphere*, **186**(6), 132-139. http://doi.org/10.1016/j.chemosphere.2017.07.038.

Yusoff, A.H., Salimi, M.N. and Jamlos, M.F. (2018), "A review: Synthetic strategy control of magnetite nanoparticles production", *Adv. Nano Res.*, **6**(1), 1-19. http://doi.org/10.12989/anr.2018.6.1.001.

CC